SnO_2/ZnO POWDERS AND THIN FILMS FOR H_2 AND NO_2 MONITORING IN WATER TREATMENT PLANTS

Yevheniia Yuzupkina[1], Tetiana Dontsova[1]

[1]National Technical University of Ukraine "Igor Sikorsky Kyiv Polytechnic Institute", Ukraine

yuzupkina.yevhenia@gmail.com

DOI: https://doi.org/10.20535/2218-930022024326244

Water treatment plants often use technologies associated with the emission of various gases. These can be anaerobic digestion processes, various methods of converting waste from wastewater treatment plants into valuable resources such as biogas. Increasingly, in order to comply with the principles of a circular economy, in to water purification additional processes such as electrolysis are carried out to obtain green hydrogen. Sometimes the preparation of drinking water itself requires a clean gas environment. Metal oxide semiconductor (MOS) gas sensors are used to monitor air at water objects and treatment plants. The work is devoted to studying the properties of SnO_2/ZnO powders and thin films with different molar ratios for monitoring hydrogen and nitrogen (IV) oxide. To characterize SnO_2/ZnO powders, X-ray phase and X-ray structural analyses were performed, diffuse reflection spectra were obtained in the UV-visible range, the band gap energy was calculated, and porosity and specific surface area were determined. Powder diffraction patterns were obtained for which the crystallite size was determined depending on the SnO_2/ZnO molar ratio. The band gap values range from 3.0 to 3.49 eV depending on the crystallite size. The most developed porous structure is 63.2 m^2/g in a powder with 60% SnO_2, in which the average pore size is about 8.5 nm. To study the response of the synthesized thin films to hydrogen and nitrogen (IV) oxide, impedance spectroscopy was performed in a closed system without access to moisture at room temperature under the influence of ultraviolet radiation. The highest response value to NO_2 is observed for the film with a molar ratio of SnO_2 to ZnO as 4 to 1 (80%/20%), which is at the level of 2.12. The highest response to hydrogen is 2.42 and corresponds to a sensitive material consisting of 100% SnO_2.

Keywords: *hydrogen, metal oxide gas sensor, nitrogen dioxide, tin (IV) oxide, water electrolysis, zinc oxide*

Received: 15 November 2024 Revised: 10 December 2024 Accepted: 15 December 2024

1. Introduction

Drinking water shortages are observed in many countries, so technologies for drinking water purification and wastewater treatment are very important and are constantly being improved. However, they are often associated with environmental pollution. Various measures are proposed for environmental safety, including methods of the circular economy. There are various proposals for the reuse of sewage sludge (Nguyen et al., 2022), reducing greenhouse gas emissions and resource recovery (Faragò et al., 2021), improving energy economy by extracting hydrogen from water treatment (Donald et al., 2023).

It is necessary to monitor not only the amount of solid waste, but also the concentration of released gases. Anaerobic digestion is often used in wastewater treatment plants to stabilize sludge, which is a natural process in which microorganisms break down organic matter in the absence of air. The result is the formation of biogas. If the process conditions are unstable or change due to certain factors, hydrogen is released as a by-product (González et al., 2023). However, hydrogen is an explosive gas, therefore

controlling its leaks is an important safety issue.

The circular economy plays an important role in water treatment. Increasingly, treatment plants are being combined with additional production of renewable energy sources. For example, recently, water electrolysis has been used for green hydrogen production in wastewater treatment processes (M. de Araujo et al., 2024). Another study reports on the production of bio-hydrogen from wastewater treatment plants by using various microorganisms in biophotolysis and photofermentation processes (Barghash et al., 2022). In other situations, in countries with poor water resources, it is proposed (Kaplan et al., 2023) to extract water from atmospheric air, which in industrial regions can be contaminated with volatile organic compounds, SO_2, NO_2, etc. Thus, monitoring of gases in the air is also important for technological processes of water extraction and purification.

Monitoring of air composition is particularly important in specific industrial wastewater treatment processes. In particular, it has been proposed (Hao et al., 2024) to carry out wet denitrification of flue gases of industrial nitrogen oxides (NO_x) in highly concentrated nitrate wastewater. They can be reduced to ammonia using electrochemical nitrate reduction reactions. In such a process, it is important to control complete denitrification and monitor toxic gas emissions.

Gas sensors are one of the promising methods of air monitoring. In water treatment, electrochemical, optical, surface acoustic wave (SAW), thermal conductivity gas sensors, quartz crystal microbalance and metal oxide semiconductor (MOS) gas sensors are used (Yadav and Indurkar, 2021).

Metal oxide sensors are not only portable and cheap, but also have a short response and recovery time, which is important in work safety with such explosive and toxic gases as H_2 and NO_2, respectively. The operation principle is based on the interfacial interaction of the analyzed gas and a semiconductor sensitive layer, the resistance of which changes as a result of the reaction. The signal is converted into an electrical one, which allows to record the response to a specific gas (Isaac et al., 2022). SnO_2, ZnO, In_2O_3, TiO_2, WO_3, CuO, etc. are often used as a sensitive material (Tereshkov et al., 2024).

The aim of this work is to synthesize SnO_2/ZnO-based powders and thin films and their characterization, to investigate the response of the SnO_2/ZnO sensitive layer to hydrogen and nitrogen (IV) oxide for air monitoring applications in water purification systems.

2. Materials and Methods

2.1 Materials

Powder synthesis: tin (II) chloride dihydrate $SnCl_2 \cdot 2H_2O$, zinc nitrate hexahydrate $Zn(NO_3)_2 \cdot 6H_2O$, methanol, 25% ammonium hydroxide solution.

Thin film synthesis: tin (II) chloride dihydrate $SnCl_2 \cdot 2H_2O$, zinc nitrate hexahydrate $Zn(NO_3)_2 \cdot 6H_2O$, citric acid, distilled water, ethylene glycol, 65% nitric acid solution.

All reagents have 99.9–99.99 wt % purity.

To test the sensitive properties of the synthesized thin films, a calibration gas mixture NO_2–N_2 with a volume fraction of nitrogen (IV) oxide of 433 ppm and a calibration gas mixture H_2–N_2 with a volume fraction of hydrogen of 20100 ppm were used.

Thin films were deposited on sital substrates with nickel contacts.

2.2 Synthesis methods of powders and thin films

The synthesis of powders of tin (IV) oxide with different molar ratios of zinc oxide was carried out according to the (Htun et al., 2023). Tin (II) chloride dihydrate and zinc nitrate hexahydrate were weighed in the corresponding molar ratios, calculated on a total amount of substance of 0.02 mol (Table 1).

Table 1. *Molar composition of salts in solution*

Sample number	**$SnCl_2 \cdot 2H_2O$**	**$Zn(NO_3)_2 \cdot 6H_2O$**
1	100 %	0 %
2	80 %	20 %
3	60 %	40 %
4	50 %	50 %
5	40 %	60 %
6	20 %	80 %
7	0 %	100 %

$37 \cdot 10^{-3}$ l of methanol were added to the corresponding salt samples. They were stirred for 5 min on a magnetic stirrer. After that, the transparent colorless solutions were mixed and the stirring was continued at a temperature of 60 ºC for 1 h. At the same time, ammonia solution was gradually added using a Pasteur pipette at a rate of 10 drops/min until the pH of the solution was 8. The resulting gels were dried at a temperature of 100 ºC until completely dry. After that, the dried powders were calcined in a crucible for 60 min at a temperature of 550 ºC.

The deposition of thin films was carried out with a similar composition to Table 1. The required amount of $SnCl_2 \cdot 2H_2O$ and $Zn(NO_3)_2 \cdot 6H_2O$ salts was weighed so that their total or individual amount of substance was 0.02 mol. In addition, 3.8425 g of citric acid were weighed. These substances were dissolved in $5 \cdot 10^{-3}$ l of distilled water. After complete dissolution, 10 cm^3 of ethylene glycol were added. In addition, $1.4 \cdot 10^{-3}$ l of a 65% nitric acid solution was added. This mixture was heated at 70 °C for 30 min. After cooling the solution to room temperature, a viscous solution was applied with a 50 µl pipette to a substrate previously washed with isopropyl alcohol and placed in a spin-coater. Rotation was carried out for 15 seconds. After that, the samples were dried for 30 min at a temperature of 100 °C. The dried substrates were calcined at 450 °C to obtain thin films.

2.3 Powders characterization and thin films physical properties analysis

X-ray diffraction was used to analyze the composition and structural properties of the powders. Data were collected by Rigaku Ultima IV diffractometer (Japan) with monochromatized CuKα radiation (20-60 kV, 2-60 mA) in the 2θ range of 20°–70° at a rate of 1 deg./min.

To determine the band gap width, UV-visible diffuse reflectance spectra were obtained using a SHIMADZU UV-3600 UV-Vis-NIR spectrophotometer (Japan). Accordingly, the band gap energy (E_g) for the powders was determined by constructing a graphical dependence, where hν (Planck's constant and photon frequency, respectively) is plotted on the abscissa axis and $(F(R)h\nu)^{1/2}$ is plotted on the ordinate axis.

The analysis of porosity and specific surface area of synthesized SnO_2/ZnO powders was carried out using low-temperature nitrogen adsorption/desorption on the surface

area and porosity analyzer JWGB Meso 112, manufactured by JWGB SCI. & TECH. (PRC).

The impedance dependence of the sensitive layers of the substrates on the frequency was determined using the electrochemical impedance analyzer VersaSTAT3 from Princeton Applied Research (United States).

3. Results and Discussion

Analysis of the powder structure by X-ray diffraction is presented in the following diffraction pattern (Fig. 1).

It was found that for pure tin (IV) oxide all peaks correspond to cassiterite. With increasing zinc oxide content in the powders, a decrease in the intensity of SnO_2 peaks and an increase in the intensity of ZnO peaks are observed.

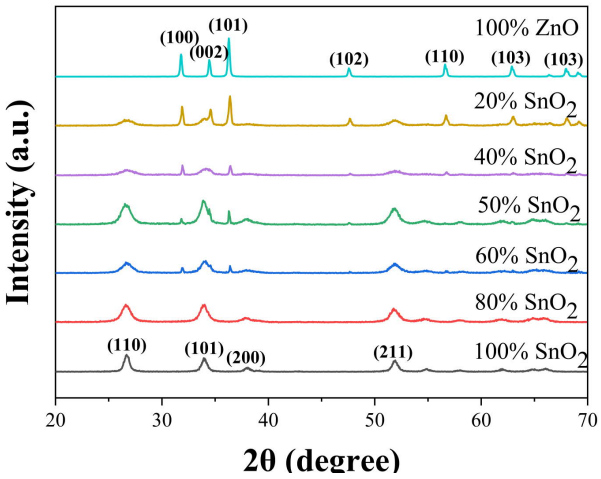

Fig.1. *Diffraction patterns of SnO_2/ZnO powders*

The structural characteristics of the obtained powders are given in Table 2.

With a molar content of tin (IV) oxide of 60% and 40% of zinc oxide, the formation of zincite crystals is observed, which explains the increased size of crystallites in these samples.

Table 2. *Size of SnO_2 and ZnO crystallites in powders*

SnO_2 content, mol.%	**Crystallite size, A**	
	Cassiterite (SnO_2)	**ZnO**
100	126	-
80	68	27
60	63	1120
50	76	261
40	56	459
20	57	109
0 (100% ZnO)	-	437

Fig. 2 shows the UV-visible diffuse reflectance spectra. It is observed that pure SnO_2 and ZnO powders have comparatively lower reflectance spectra.

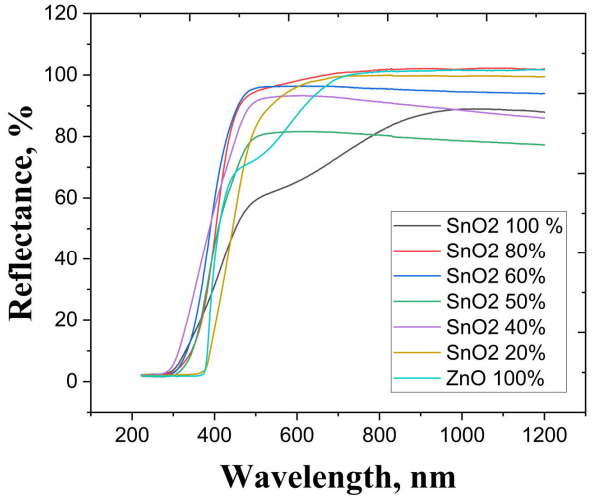

Fig. 2. *Obtained UV-vis diffuse reflectance spectra*

Tin (IV) oxide has a band gap of 3.6 eV (Jithin et al., 2021). The band gap width for powders with different SnO_2 contents was determined by converting the diffuse reflection spectrum into an absorption spectrum using the Kubelka-Munk theory. The band gap energy (E_g) for the powders was determined by plotting $(F(R)h\nu)^{1/2}$ versus $h\nu$. (Motsoeneng et al., 2023). By extrapolating the obtained graphs, the band gap energy value was

determined for each powder (Table 3). The measurement error in this study is due to the error of the spectrophotometer used. In particular, the photometric accuracy is ± 0.003 Abs (at 1 Abs); ± 0.002 Abs (at 0.5 Abs). This has a minor impact on the results obtained.

Table 3. *Band gap of SnO_2/ZnO powders*

SnO_2 content, mol.%	**The band-gap energy, eV**
100	3.29
80	3.04
60	3.34
50	3.24
40	3.49
20	3.0
0 (100% ZnO)	3.14

Thus, the band gap for different contents of tin (IV) oxide varies from 3.0 to 3.49 eV. For comparison, in the literature there is information about the experimentally obtained band gap values of pure SnO_2 (3.45 eV) and ZnO (3.23 eV), as well as the SnO_2/ZnO composite in a molar ratio of 1:1 (3.40 eV) (Hamrouni et al., 2013). These data differ from the results obtained in this study. At the same time, a similar trend is observed to decrease the band gap values in the following order: SnO_2, SnO_2/ZnO, ZnO. The differences in results can be explained by the fact that the band gap of semiconductors increases with decreasing particle size due to the quantum size effect. The same thing happens in the case of the surface to volume ratio (Ali et al., 2022).

In order to obtain information about the porosity and specific surface area of the synthesized SnO_2/ZnO powders, low-temperature adsorption/desorption of nitrogen was carried out. All the obtained isotherms have type V adsorption isotherms according to the IUPAC classification (Thommes, 2016), which indicates a microporous or macroporous adsorbent with relatively weak interactions with the adsorbate.

The obtained analysis results are contained in Table 4. It is observed that powders containing pure SnO_2 and ZnO have the smallest surface area and the largest pore size. The most developed surface area by BET of 63.2 m^2/g is found in the powder containing 60% SnO_2 and 40% ZnO. The measurement accuracy of the porosity analyzer is ±1% in the specific surface area measurement range. Analytical balances with a resolution of 0,003 were also used for sampling.

Measurements to characterize the obtained samples were carried out at least twice. Moreover, the results did not differ significantly, which indicates the reliability of the obtained data.

Table 4. *Results of porosity and specific surface area analysis of SnO_2/ZnO powders*

SnO_2 content, %	**Type of adsorption isotherm**	**Surface area (BET), m^2/g**	**Total pore volume, cm^3/g**	**Average pore size, nm**
100	V	24.1	0.103	17.1
80		52.1	0.086	6.6
60		63.2	0.135	8.5
50		58.9	0.138	9.3
40		38.8	0.161	16.6
20		38.6	0.164	17.0
0		6.0	0.042	27.8

Measurements of the impedance versus frequency of sensitive layers based on SnO_2/ZnO were carried out in air, using ultraviolet irradiation, and in an environment of the detected gas simultaneously with UV radiation. Impedance spectroscopy was performed in a closed system without access to moisture at room temperature (~18 °C).

The response of substrates with a sensitive layer to an oxidizing gas such as NO_2 can be estimated using the equation (Balasubramani et al., 2020; Xu and Ho, 2017):

$$R_{ox.g.} = \frac{|Z|_g}{|Z|_a},$$

where $|Z|_g$ is the gas impedance, MΩ; $|Z|_a$ is the air impedance, MΩ.

The response of substrates with a sensitive layer to a reducing gas (H_2) is described by the equation:

$$R_{red.g.} = \frac{|Z|_a}{|Z|_g}.$$

The results of the study of the impedance of thin films under nitrogen (IV) oxide impact are given in Table 5. For all samples, with increasing frequency, a decrease in the impedance value is observed, which is associated with the excitation of charge carriers under the action of an electric field. This promotes their movement through the nanocomposite structure, increasing the conductivity and reducing the impedance of the system (Zankat et al., 2021). When using a UV lamp, the impedance in all cases decreases, which is also explained by the activation of additional charge carriers due to the excitation of electrons from the valence band to the conduction band under the influence of ultraviolet radiation.

Table 5. *Impedance value and NO_2 response*

Sample number	Composition of the sensitive layer SnO_2/ZnO	Impedance value, MΩ			Sensitive layer response ($R_{ox.g.}$)
		In the air	Under UV irradiation	In NO_2 and UV radiation	
1	100%/0%	1.84	1.42	1.73	1.22
2	80%/20%	2.39	0.86	1.82	2.12
3	60%/40%	1.44	1.13	1.53	1.35
4	50%/50%	1.96	1.10	0.91	0.83
5	40%/60%	1.89	0.85	1.18	1.39
6	20%/80%	2.04	1.15	0.81	0.70
7	0%/100%	1.77	1.00	1.48	1.48

Since SnO_2 and ZnO are sensitive *n*-type materials, when the system is exposed to an oxidizing gas such as nitrogen (IV) oxide, an increase in resistance is observed (Xu and Ho, 2017). This prediction holds for samples 1–3, 5 and 7, where the molar fraction of SnO_2 varies from 0.02 to 0.008 mol or where this oxide is absent altogether (sample 7). The increased content of SnO_2 nanoparticles provides improved conductivity and, therefore, a decrease in impedance in the system with a higher content of nanoparticles (Zankat et al., 2021). This can be explained by the improved number of crystallite boundaries in nanocomposites with a higher content of SnO_2 nanoparticles. They contain a large number of

defects, in particular oxygen vacancies, which are characterized by increased disorder in the boundary zones compared to the crystalline core. With an increase in the total concentration of crystallite boundaries, the number of defects, the level of disorder and the concentration of oxygen vacancies increase. Such vacancies act as charge carrier donors, generating free carriers that move through the lattice, contributing to the conductivity of the nanocomposite material.

According to the results of Table 5, the best substrate response to the oxidizing gas nitrogen (IV) oxide with a concentration of 433 ppm is the sensitive layer with a molar ratio of SnO_2 to ZnO equal to 80%/20%.

Similar measurements of the impedance dependence on the frequency of the sensitive layers of the sensor based on SnO_2/ZnO were carried out using ultraviolet irradiation and in a hydrogen environment simultaneously (Table 6).

In comparison with previous measurements, with increasing frequency, a decrease in the impedance value is also observed, as with the influence of ultraviolet irradiation. Since hydrogen is a reducing gas, and the sensitive layers based on SnO_2 and ZnO are n-type materials, in the case of using UV radiation and hydrogen, the impedance decreases. With an increase in the zinc oxide content in the samples, the value of the complex resistance for all measurements also increases. The average impedance value in an environment with H_2 was determined for each sample.

Table 6. *Impedance value and H_2 response*

Sample number	**Composition of the sensitive layer SnO_2/ZnO**	**Impedance value, MΩ**			**Sensitive layer response ($R_{red.g.}$)**
		In the air	**Under UV irradiation**	**In H_2 and UV radiation**	
1	100%/0%	64.54	2.03	0.84	2.42
2	80%/20%	623	14.4	12.8	1.13
3	60%/40%	823	36.51	26.68	1.37
4	50%/50%	698	108	70.36	1.53
5	40%/60%	421	94.78	97.87	0.97
6	20%/80%	424	83.54	67.14	1.24
7	0%/100%	374	110	72.81	1.51

According to the analysis results, the best response to hydrogen is given by a substrate with a molar content of tin (IV) oxide of 100%.

It is worth noting that the study was conducted in a closed system where gas was supplied. However, in real systems, moisture may be present, which can significantly affect the sensor response. To prevent this in high humidity conditions, a sampling design can be proposed that will first be supplied to a dryer and then to the gas sensor.

To compare the obtained responses of the sensitive layers and the efficiency of their use, the response of sensors to NO_2 and H_2 in existing studies is shown in Table 7.

From the above information it is clear that there are few studies on the influence of the composition of SnO_2/ZnO thin film on the sensor response. Moreover, they all differ in

the process conditions (concentration of the analyzed gas and process temperature), as well as in factors such as the materials used (type and material of the substrate contacts).

Table 7. *Comparison of hydrogen and nitrogen dioxide gas sensors*

Thin film	Sensing gas	Operating conditions	Response	Reference
SnO_2/ZnO (Sn:Zn=1:1)	30 ppm H_2	T = 200 °C	93	(Zhang et al., 2023)
0,1 SnO_2 loaded ZnO NFs	0.05 ppm H_2	T = 300 °C	50,1	(Lee et al., 2019)
ZnO/SnO_2 NF (Zn:Sn =1:1)	10 ppm NO_2	T = 350 °C	109	(Phuoc et al., 2021)
SnO_2/ZnO (Sn:Zn=20:1)	0.05 ppm NO_2	T~20 °C	336 %	(Guo et al., 2021)

Therefore, this study is new and offers previously unexplored aspects of the comparison of the composition of SnO_2/ZnO of the sensitive layer and the sensor response. The sensor response can be improved in future studies by introducing new conditions (doping with a noble metal, using elevated sensing temperatures).

4. Conclusions

Air monitoring at water treatment facilities and structures associated with them is necessary to control the leakage of gases such as H_2 and NO_2. For this purpose, metal oxide semiconductor gas sensors can be used.

To characterize SnO_2/ZnO composites, X-ray phase and X-ray structural analysis were performed, UV-visible diffuse reflectance spectra were obtained, porosity and specific surface area were determined.

The obtained results are reliable, since the error of the measurements is determined by the error of the analytical instruments used, which is insignificant. In addition, the characterization of the samples was carried out twice, which confirmed the reproducibility of the results.

XRD analysis confirmed the presence of cassiterite and zinc oxide in the synthesized powders. The size of the crystallites of the material varies nonlinearly depending on the added amount of ZnO. The band gap value ranges from 3.0 to 3.49 eV, which may depend on the size of the crystallites. The results of nitrogen adsorption/desorption showed that an increase in the ZnO content contributes to the formation of a more developed porous structure and has a maximum of 63.2 m^2/g at 60% SnO_2.

Impedance spectroscopy was performed to determine the response of the synthesized thin films to hydrogen and nitrogen dioxide. The best response to NO_2 is 2.12 and given by a substrate with 80% of SnO_2, and to H_2 – 2.42 by a 100% of SnO_2.

However, water treatment plants and related facilities have a high level of humidity. This can significantly affect the operation of a metal-oxide semiconductor sensor. Therefore, in further studies, it is planned to observe the effect of humidity on the response of the SnO_2/ZnO sensitive layer of the sensor.

Acknowledgment

We are grateful to the Ministry of Education and Science of Ukraine for funding the PH/51-2024 project.

References

1.Ali, S. I.; Dutta, D.; Das, A.; Mandal, S.; Chandra Mandal, A. Understanding the Structure-Property Correlation of Tin Oxide Nanoparticles Synthesized Through the Sol-Gel Technique. *J. Lumin.* **2022**, 119465. https://doi.org/10.1016/j.jlumin.2022.119465.

2.Balasubramani, V.; Chandraleka, S.; Rao, T. S.; Sasikumar, R.; Kuppusamy, M. R.; Sridhar, T. M. Review—Recent Advances in Electrochemical Impedance Spectroscopy Based Toxic Gas Sensors Using Semiconducting Metal Oxides. *J. Electrochem. Soc.* **2020**, *167* (3), 037572. https://doi.org/10.1149/1945-7111/ab77a0.

3.Barghash, H.; AlRashdi, Z.; Okedu, K. E.; Desmond, P. Life-Cycle Assessment Study for Bio-Hydrogen Gas Production From Sewage Treatment Plants Using Solar PVs. *Energies* **2022**, *15* (21), 8056. https://doi.org/10.3390/en15218056.

4.Donald, R.; Boulaire, F.; Love, J. G. Contribution to Net Zero Emissions of Integrating Hydrogen Production in Wastewater Treatment Plants. *J. Environ. Manag.* **2023**, *344*, 118485. https://doi.org/10.1016/j.jenvman.2023.118485.

5.Faragò, M.; Damgaard, A.; Madsen, J. A.; Andersen, J. K.; Thornberg, D.; Andersen, M. H.; Rygaard, M. From Wastewater Treatment to Water Resource Recovery: Environmental and Economic Impacts of Full-Scale Implementation. *Water Res.* **2021**, *204*, 117554. https://doi.org/10.1016/j.watres.2021.117554.

6.González, J. F.; Álvez-Medina, C. M.; Nogales-Delgado, S. Biogas Steam Reforming in Wastewater Treatment Plants: Opportunities and Challenges. *Energies* **2023**, *16* (17), 6343. https://doi.org/10.3390/en16176343.

7.Guo, J.; Li, W.; Zhao, X.; Hu, H.; Wang, M.; Luo, Y.; Xie, D.; Zhang, Y.; Zhu, H. Highly Sensitive, Selective, Flexible and Scalable Room-Temperature NO2 Gas Sensor Based on Hollow SnO_2/ZnO Nanofibers. *Molecules* **2021**, *26* (21), 6475. https://doi.org/10.3390/molecules26216475.

8.Hamrouni, A.; Lachheb, H.; Houas, A. Synthesis, Characterization and Photocatalytic Activity of ZnO-SnO_2 Nanocomposites. *Mater. Sci. Eng.* **2013**, *178* (20), 1371–1379. https://doi.org/10.1016/j.mseb.2013.08.008.

9.Hao, R.; Song, Y.; Yang, L.; Guo, Y.; Wu, X.; Ma, Z.; Qian, Z.; Liu, F.; Wu, Z.; Wang, L. Electrochemical Reduction of Flue Gas Denitrification Wastewater to Ammonia Using a Dual-Defective Cu_2O@Cu Heterojunction Electrode. *Environ. Sci. & Technol.* **2024**. https://doi.org/10.1021/acs.est.3c09811.

10. Htun, H. M.; Aung, C. C. H.; May, A. C.; Aung, T. H. Structural and Morphological Properties of ZnO-SnO_2 Nanocomposite by Sol-Gel Method. *Hinthada Univ. Res. J.* **2023**, *13* (2), 56–64.

11. Isaac, N. A.; Pikaar, I.; Biskos, G. Metal Oxide Semiconducting Nanomaterials for Air Quality Gas Sensors: Operating Principles, Performance, and Synthesis Techniques. *Microchim. Acta* **2022**, *189* (5). https://doi.org/10.1007/s00604-022-05254-0.

12. Jithin, P. V.; Sudheendran, K.; Sankaran, K. J.; Kurian, J. Influence of Fe-Doping on the Structural and Photoluminescence Properties and on the Band-Gap Narrowing of SnO_2 Nanoparticles. *Opt. Mater.* **2021**, *120*, 111367. https://doi.org/10.1016/j.optmat.2021.111367.

13. Kaplan, A.; Ronen-Eliraz, G.; Ratner, S.; Aviv, Y.; Wolanov, Y.; Avisar, D. Impact of Industrial Air Pollution on the Quality of Atmospheric Water Production. *Environ. Pollut.* **2023**, 121447. https://doi.org/10.1016/j.envpol.2023.121447.

14. Lee, J.-H.; Kim, J.-Y.; Kim, J.-H.; Kim, S. Enhanced Hydrogen Detection in ppb-Level by Electrospun SnO2-Loaded ZnO Nanofibers. *Sensors* **2019**, *19* (3), 726. https://doi.org/10.3390/s19030726.

15. M. de Araujo, D.; Barbosa Segundo, I. D.; Cardozo, J. C.; Santos, J. E. L.; Nascimento, J. H. O.; Gondim, A. D.; dos Santos, E. V.; Martínez-Huitle, C. A. Produced Water Electrolysis With Simultaneous Green H_2 Generation: From Wastewater to the Future of the Energetic Industry. *Fuel* **2024**, *373*, 132369. https://doi.org/10.1016/j.fuel.2024.132369.

16. Motsoeneng, R. G.; Swart, H. C.; Motaung, D. E. The Influence of Fe Loading on the Optical and Gas Sensing Characteristics of SnO_2/ZnO Heterostructures. *Phys. B* **2023**, *668*, 415256. https://doi.org/10.1016/j.physb.2023.415256.

17. Nguyen, M. D.; Thomas, M.; Surapaneni, A.; Moon, E. M.; Milne, N. A. Beneficial

Reuse of Water Treatment Sludge in the Context of Circular Economy. *Environ. Technol. & Innov*. **2022**, 102651. https://doi.org/10.1016/j.eti.2022.102651.

18. Phuoc, P. H.; Viet, N. N.; Thong, L. V.; Hung, C. M.; Hoa, N. D.; Duy, N. V.; Hong, H. S.; Hieu, N. V. Comparative Study on the Gas-Sensing Performance of ZnO/SnO_2 External and ZnO–SnO_2 Internal Heterojunctions for ppb H_2S and NO2 Gases Detection. *Sens. Actuators B* **2021**, *334*, 129606. https://doi.org/10.1016/j.snb.2021.129606.

19. Tereshkov, M.; Dontsova, T.; Saruhan, B.; Krüger, S. Metal Oxide-Based Sensors for Ecological Monitoring: Progress and Perspectives. *Chemosensors* **2024**, *12* (3), 42. https://doi.org/10.3390/chemosensors12030042.

20. Thommes, M. Physisorption of Gases, With Special Reference to the Evaluation of Surface Area and Pore Size Distribution (IUPAC Technical Report). *Chem. Int.* **2016**, *38* (1), 25. http://dx.doi.org/10.1515/pac-2014-1117.

21. Xu, F.; Ho, H.-P. Light-Activated Metal Oxide Gas Sensors: A Review. *Micromachines* **2017**, *8* (11), 333. https://doi.org/10.3390/mi8110333.

22. Yadav, A.; Indurkar, P. D. Gas Sensor Applications in Water Quality Monitoring and Maintenance. *Water Conserv. Sci. Eng.* **2021**, *6* (3), 175–190. https://doi.org/10.1007/s41101-021-00108-x.

23. Zankat, A.; Gadani, K.; Vadgama, V.; Udeshi, B.; Gal, M.; Solanki, S.; Vaishnani, A.; Shrimali, V. G.; Solanki, P. S.; Shah, N. A.; et al. Frequency and Temperature Dependent Electrical Properties of ZnO–SnO_2 Nanocomposites. *Phys. B* **2021**, *617*, 413140. https://doi.org/10.1016/j.physb.2021.413140.

24. Zhang, X.-Y.; Ren, Q.; Wang, C.; Zhu, L.; Ding, W.-J.; Cao, Y.-Q.; Li, W.-M.; Wu, D.; Li, A.-D. Atomic Layer Deposited SnO2/ZnO Composite Thin Film Sensors With Enhanced Hydrogen Sensing Performance. *Appl. Surf. Sci*. **2023**, 157973. https://doi.org/10.1016/j.apsusc.2023.157973.

SnO_2/ZnO ПОРОШКИ ТА ТОНКІ ПЛІВКИ ДЛЯ МОНІТОРИНГУ H_2 ТА NO_2 НА ВОДООЧИСНИХ СТАНЦІЯХ

Євгенія Юзупкіна[1], Тетяна Донцова[1]

[1] Національний технічний університет України

«Київський політехнічний інститут імені Ігоря Сікорського», Україна

yuzupkina.yevhenia@gmail.com

Станції очищення води часто використовують технології, пов'язані з викидом різних газів. Це можуть бути процеси анаеробного зброджування, різні методи перетворення відходів очисних станцій на цінні ресурси типу біогазу. Все частіше з метою дотримання принципів циклічної економіки окрім очищення води проводять додаткові процеси типу електролізу для отримання зеленого водню. Іноді сама підготовка питної води потребує чистого газового середовища. З метою моніторингу повітря на водних об'єктах та очисних станціях використовують металоксидні напівпровідникові газові сенсори. Роботу присвячено дослідженню властивостей SnO_2/ZnO порошків та тонких плівок із різним мольним співвідношенням для моніторингу водню та нітроген (IV) оксиду. Для характеризації порошків SnO_2/ZnO було проведено рентгенофазовий та рентгеноструктурний аналізи, отримано спектри дифузного відбиття в УФ-видимому діапазоні, обчислено ширину забороненої зони, визначено пористість та питому поверхню. Отримано дифрактограми порошків, для яких визначено розмір кристалітів в залежності від мольного співвідношення SnO_2/ZnO. Значення ширини забороненої зони коливаються в діапазоні від 3,0 до 3,49 еВ в залежності від розміру кристалітів. Найрозвиненіша пориста структура 63,2 $м^2/г$ у порошку з 60 % SnO_2, у якому середній розмір пор близько 8,5 нм. Для дослідження відгуку синтезованих тонких плівок на водень та нітроген (IV) оксид було проведено імпедансну спектроскопію в закритій системі без доступу вологи за кімнатної температури під впливом ультрафіолетового випромінювання. Найбільше значення відгуку до NO_2 спостерігається для плівки із мольним співвідношенням SnO_2 до ZnO як 4 до 1 (80%/20%), який є на рівні 2,12. Найбільший відгук по відношенню до водню становить 2,42 і відповідає чутливому матеріалу, що складається з 100 % SnO_2.

Ключові слова: *водень, електроліз води, метал оксидний газовий сенсор, нітроген діоксид, станум (IV) оксид, цинк оксид*